

# The Effects of Policy Uncertainty and Risk Aversion on Carbon Capture, Utilization, and Storage Investments

Connor Colombe\*, Benjamin D. Leibowicz, and Benjamin R. Mendoza

*Operations Research and Industrial Engineering, The University of Texas at Austin*

Last updated: October 2, 2023

## Abstract

Many model-based decarbonization pathways include substantial carbon capture, utilization, and storage (CCUS), and engineering cost estimates suggest that these technologies should be profitable to deploy under current incentives, such as the 45Q tax credits in the United States. However, CCUS investments have been slow to materialize. In this paper, we investigate the extent to which policy uncertainty and investor risk aversion may explain the limited buildout of CCUS infrastructure to date. To do so, we develop a two-stage stochastic programming model for optimal CCUS infrastructure network design that incorporates policy uncertainty and risk aversion as novel features. We then apply it to an empirically parameterized case study of the Texas-Louisiana Gulf Coast region. Our results show that the current 45Q incentive levels make a fair number of CCUS projects profitable even if they were to be discontinued after ten years. Therefore, while future policy uncertainty reduces CCUS development, the maximum effect size is only a 7% decline in expected total CO<sub>2</sub> captured. Interestingly, more significant risk aversion could accelerate CCUS investment since a more risk-averse investor prefers to fully exploit the current, known incentives rather than preserve CO<sub>2</sub> storage capacity for future, unknown incentives.

## 1 Introduction

Carbon capture, utilization, and storage (CCUS) refers to the collection of technologies and processes that capture carbon dioxide (CO<sub>2</sub>), transport it across space, and either utilize it as an input to production processes or deposit it into geologic storage. CCUS is attractive because it reduces carbon emissions to the atmosphere without reducing fossil fuel use and because it can be deployed in many sectors, including some – such as heavy industry – in which switching to renewable energy is difficult and/or expensive at present. Decarbonization pathways produced using energy-economy and integrated assessment models foresee CCUS playing a major role in reducing economy-wide greenhouse gas (GHG) emissions in the United States (U.S.) ([Electric Power Research Institute, 2022](#); [White House, 2021](#)) and globally ([IPCC, 2022](#)). However, despite the key role envisioned for CCUS in the energy transition,

---

\*Corresponding author. Email address: [cco1ombe@utexas.edu](mailto:cco1ombe@utexas.edu).

large-scale CCUS projects have been slow to materialize. As of September 2022, 40 large-scale CCUS facilities are operating worldwide, with around 200 more in development ([Global CCS Institute, 2022](#)). Historically, most CCUS projects in the U.S. have been initiated to capture CO<sub>2</sub> and utilize it for enhanced oil recovery (EOR), whereby oil and gas producers inject CO<sub>2</sub> in order to boost fossil fuel production. However, achieving significant carbon emissions reductions via CCUS requires further incentives to make it economically viable, including for geologic storage applications.

The U.S. federal government incentivizes CCUS through the 45Q tax credit, which essentially offers firms a subsidy per ton of CO<sub>2</sub> that they capture. The level of the incentive depends on whether the CO<sub>2</sub> is utilized for industrial production or injected into geologic storage, with the latter earning a higher subsidy. The 45Q tax credit was first introduced in 2008 and the levels of its incentives have been adjusted several times since then. Most recently, the Inflation Reduction Act of 2023 increased the tax credits to \$60 and \$85 per ton of CO<sub>2</sub> utilized or geologically stored, respectively. These incentive level adjustments were complemented by other legislative changes designed to provide broader access to these incentives. The current 45Q incentive values represent a substantial commitment to supporting the deployment of CCUS technologies in the U.S.

While the importance of CCUS for economy-wide decarbonization has been recognized for years and significant policy incentives for its deployment exist in the U.S., investments in CCUS infrastructure to date have been limited. This is the case despite analyses suggesting that a large number of CCUS projects should be profitable at the current 45Q incentive levels, based on bottom-up engineering cost estimates ([Waxman, Corcoran, Robison, Leibowicz and Olmstead, 2021](#)). One hypothesis for the slow rate of CCUS infrastructure deployment observed in practice focuses on the role of policy uncertainty. In order to justify incurring a large, upfront, fixed cost to invest in CCUS infrastructure, firms need to be confident that they can continue to earn revenues – for example, through the 45Q tax credits – for the CO<sub>2</sub> that they capture over many years. If firms base their investment decisions on a substantial degree of risk aversion, then the dampening effect of future policy uncertainty on their CCUS investments could be even larger. In this paper, our goal is to investigate this hypothesis and address two interrelated research questions: (1) To what extent does policy uncertainty diminish CCUS infrastructure investments? (2) How does the effect of policy uncertainty on CCUS investments depend on the degree of investor risk aversion?

To answer these questions, we develop a model for CCUS infrastructure network optimization that is distinct from existing models in two respects that are relevant to our research questions. First, we formulate the model as a two-stage stochastic program in which policy incentive levels are known in the first stage but uncertain in the second stage. To make optimal first-stage investment decisions, the model hedges against all of the potential second-stage incentive levels while considering the recourse decisions that it could implement in the second stage. Second, we incorporate a risk-averse objective function that allows us to define scenarios where investors are risk-averse. This enables us to go beyond standard linear formulations that inherently assume that decision-making is risk-neutral. We then apply our stochastic optimization model to a case study of the Texas-Louisiana Gulf

Coast, parameterized using empirical data on large point sources of CO<sub>2</sub> and candidate CO<sub>2</sub> pipeline segments established via geographic information system (GIS) data analysis. By comparing the results of scenarios with different probability distributions over second-stage incentive levels and degrees of risk aversion, we obtain insights into the effects of policy uncertainty and risk aversion on CCUS investments.

For our case study, we find that greater policy uncertainty tends to reduce total first-stage investments in CCUS infrastructure as well as the total amount of CO<sub>2</sub> captured (in expectation) over the modeled timeframe. Interestingly, we see that a higher degree of risk aversion often leads to more CCUS infrastructure investment in the first stage, rather than less as one might expect. The mechanism seems to be that the current 45Q incentive levels are sufficient to justify a substantial amount of CCUS deployment; by investing now instead of later, a risk-averse investor can take advantage of the known incentive levels in the near-term instead of gambling on the unknown future incentive levels. The intertemporal capacity constraints on the total amounts of CO<sub>2</sub> that can be geologically stored at the most advantageous storage locations heighten the tradeoff between capturing more CO<sub>2</sub> in the first or second stage.

The remainder of this paper is structured as follows. In Section 2 we review the most relevant literature and position our study relative to prior work. In Section 3 we present our optimization model and describe how we parameterize a case study of the Texas-Louisiana Gulf Coast. We present and discuss our case study results in Section 4. We conclude the paper in Section 5 with a summary of our main findings, model limitations, and future research directions.

## 2 Literature review

### 2.1 The role of CCUS in decarbonization pathways

There is a large literature that emphasizes the important role that CCUS technologies ought to play – or need to play, depending on the analysis – in order to achieve ambitious decarbonization goals. The Sixth Assessment Report of the Intergovernmental Panel on Climate Change (IPCC) contends that nearly all climate change mitigation pathways that limit global warming to within 1.5°C involve the implementation of CCUS. Furthermore, geologic CO<sub>2</sub> storage may need to be employed on the scale of 350 billion to 1 trillion cumulative metric tons of CO<sub>2</sub> by 2050 in order to achieve that global warming target (IPCC, 2022). In the U.S., the Council on Environmental Quality (White House, 2021) notes that in order to reach the current administration’s ambitious climate goals, CO<sub>2</sub> must be sequestered in significant quantities. Indeed, the White House (2021) asserts that despite the U.S. having more CCUS projects planned and proposed than any other country, to reach its climate reduction goals, CCUS deployment in the U.S. needs to increase tenfold in the next decade. They also note the growing scientific consensus around the importance of CCUS technology and that the U.S. can play a pivotal role in driving down the technology costs, thus accelerating CCUS deployment around the globe.

The power sector is an immediate focus of deep decarbonization pathways. Rogelj, Luderer, Pietzcker, Kriegler, Schaeffer, Krey and Riahi (2015) argue that the first step in transforming the global energy system to limit global warming to 1.5°C or less is a comprehensive decarbonization of electricity. In their analysis, in scenarios that are consistent with the 1.5°C goal, global CO<sub>2</sub> emissions become net-zero or net-negative around 2050. Negative emissions are achieved primarily via bioenergy with CCS (BECCS). The authors contend that BECCS or other CO<sub>2</sub> removal technologies are indispensable in the latter half of the twenty-first century for 1.5°C scenarios. Kriegler, Weyant, Blanford, Krey, Clarke, Edmonds, Fawcett, Luderer, Riahi, Richels, Rose, Tavoni and Van Vuuren (2014) present a synthesis of results from the Stanford Energy Modeling Forum 27 Study. They specifically investigate the importance of individual mitigation options for the feasibility of climate targets and the cost of achieving them. To remain below 450 ppm CO<sub>2</sub> by 2100, CCS technologies play crucial roles because they can be applied to multiple sectors to decouple fossil fuel use and emissions and can be deployed in applications such as BECCS that produce net-negative emissions. Wang, Chen, Zhang and Li (2020) corroborate these points in the context of China. They show that CCS deployment is essential for enabling China to decarbonize its power sector without turning its many coal power plants into stranded assets, and that BECCS should also be implemented as part of a strategy aligned with the 2°C goal. The key role of CCUS in power sector decarbonization has also been highlighted in the U.S. context. Indeed, in the U.S. Mid-Century Strategy for Deep Decarbonization, the baseline scenario gradually eliminates almost all fossil fuel-based power plants lacking CCUS by the year 2050 (White House, 2016). The International Energy Agency (2020) argues that CCUS should play a prominent role in the transition to low-carbon power generation while meeting strong growth in power demand. They suggest that CCUS will help decarbonize electricity in three ways. First, retrofitting existing plants helps avoid the potential locked-in emissions from continuing to run existing plants for the remainders of their lifetimes. Second, to complement increased variable renewable energy generation, CCUS provides dispatchable, low-carbon generation. Third, BECCS implementation enables negative-emission power plants that can offset emissions in harder-to-abate sectors and support “net-zero” climate goals.

CCUS is likely to be especially important for decarbonizing the industrial sector, where high temperatures are required and process emissions from chemical reactions are difficult to address (White House, 2021). Luh, Budinis, Giarola, Schmidt and Hawkes (2020) present a novel simulation framework to model investment decisions in industry to quantify the effects of combined measures for CO<sub>2</sub> emissions reductions. They find that an integrated approach that utilizes fuel switching, industrial electrification, and CCS is significantly more effective than any of the three in isolation. In the “Sustainable Development Scenario” outlined in the 2019 World Energy Outlook by the International Energy Agency (2019), CCUS is applied to the power generation and industrial sectors, collectively accounting for 9% of total emissions reductions projected through 2050. According to these reports, there is a distinct recognition of the vital role that CCUS should play in deep decarbonization pathways, particularly through applications in the power and industrial sectors.

## 2.2 Optimization models for CCUS infrastructure networks

Given the importance of CCUS development and the high costs of building and operating CCUS infrastructure, there have been extensive efforts to develop models to determine the optimal configurations for CCUS infrastructure systems. The central decisions that these optimization models are designed to analyze (typically in an integrated fashion) include the following:

- Which point sources of CO<sub>2</sub> should be equipped with CO<sub>2</sub> capture and how much CO<sub>2</sub> should be captured from each one?
- Which CO<sub>2</sub> sinks should be opened and how much CO<sub>2</sub> should be stored at each of them?
- Which pipelines should be built to transport CO<sub>2</sub> from sources to sinks, how large should they be, and how much CO<sub>2</sub> should be transported through each one?

We shall refer to the problem that seeks to optimize all of these decisions in an integrated fashion as the CCUS infrastructure optimization problem. Its mix of discrete and continuous decision variables naturally lends itself to modeling the problem as a mixed-integer linear program (MILP). In this paper, we develop two MILPs for the CCUS infrastructure optimization problem that builds on a number of existing MILP models in the literature but extend them by incorporating several novel features. Before presenting our models in the next section, we highlight some of the recent work on the CCUS infrastructure optimization problem herein.

Most of the optimization models created for the CCUS infrastructure optimization problem are deterministic. [Middleton and Bielicki \(2009\)](#) developed *SimCCS*, a MILP that determines the least-cost CCUS infrastructure network for storing a targeted amount of CO<sub>2</sub>, which is exogenously specified. Their model takes as inputs sets of sources and sinks along with their locations, capacities, and associated fixed and variable costs, as well as the carbon capture goal. Unlike other models at the time, their model accounts for the relevant geography in the region where the sources and sinks reside and constructs a realistic network of candidate pipeline segments during a preprocessing stage. The model can build pipelines in several discrete sizes, with cost parameter values that reflect economies of scale in pipeline investment costs. Since this first version of *SimCCS*, researchers have continued to develop it over time. [Kuby, Bielicki and Middleton \(2011\)](#) developed *SimCCS<sup>CAP</sup>*, which modified the *SimCCS* framework to identify the profit-maximizing infrastructure design and CO<sub>2</sub> capture amounts under a given CO<sub>2</sub> emissions price. The model we develop for this study is similar to *SimCCS<sup>CAP</sup>* in that it seeks to maximize profit by capturing an endogenously determined amount of CO<sub>2</sub> that depends on how attractive the policy incentives are. [Middleton, Kuby, Wei, Keating and Pawar \(2012\)](#) further generalized the *SimCCS* framework in their extended version *SimCCS<sup>Time</sup>*. It builds out the CCUS infrastructure network over a set of multiple time periods, in contrast to the original model that is static and corresponds to some single, representative year. The representation of time periods in the *SimCCS* family of models was generalized further by [Jones, Yaw, Bennett, Ogland-Hand, Strahan and Middleton \(2022\)](#).

Beyond *SimCCS*, the literature includes several other models developed to study CCUS infrastructure optimization. [Mendelevitch, Herold, Oei and Tissen \(2010\)](#) developed a multi-period, welfare-maximizing MILP called CCTSMOD for the CCUS infrastructure optimization problem and applied it to Europe. While structurally similar to *SimCCS*, CCTSMOD represents the multi-period buildout of CCUS infrastructure (making it similar to more recent extensions of *SimCCS*) and presents the firm the option to purchase carbon certificates instead of paying to implement CCUS. That is, for a given target quantity of CO<sub>2</sub> emissions reduction, if implementing CCUS is too costly, the firm may opt to purchase carbon certificates that allow it to emit CO<sub>2</sub> instead of capturing it. [Morbee, Serpa and Tzimas \(2011\)](#) developed their *InfraCCS* tool for the problem of determining least-cost pipeline routes to populate the candidate pipeline network, which is a preprocessing step necessary to parameterize the CCUS infrastructure optimization problem. Rather than use a modified version of Dijkstra’s algorithm to generate a candidate pipeline network, they used a Delaney triangulation method and *k*-means clustering of nodes to reduce the preprocessing computational complexity and allow for the dynamic buildout of CO<sub>2</sub> pipeline infrastructure over several time periods. However, the tradeoff of reduced computational complexity is a lower-resolution network.

While the models described in the previous paragraphs are all deterministic optimization tools, there have been some efforts to incorporate uncertainty into the CCUS infrastructure optimization problem. [Middleton and Yaw \(2018\)](#) used *SimCCS* to study the impact of uncertainty in the potential geologic storage capacities of CO<sub>2</sub> storage sites. They ran a Monte Carlo-style simulation by varying the storage capacities of several storage sites and running *SimCCS* on each instance. They found that varying storage capacity assumptions can have a large effect on the resulting CCUS network for a given CO<sub>2</sub> capture target. It is important to note that, unlike our approach in this paper, [Middleton and Yaw \(2018\)](#) did not attempt to determine CCUS infrastructure configurations that hedge against different realizations of the storage capacities; instead, their Monte Carlo simulation maps various storage capacity assumptions to their corresponding optimal infrastructure designs. [Lee, Lee, Lee and Han \(2017\)](#) present a multi-objective stochastic decision-making algorithm for the design and operation of a CCUS network. In a similar vein as *SimCCS*, their problem considers building and operating a CCUS infrastructure network over a set of regions with both capture and storage facilities and transportation modes between each, all subject to a capture goal. They introduce uncertainty through two stages of decisions. In the first stage, the decision-maker faces known fixed infrastructure development costs and in the second stage, once the chosen infrastructure is built, the operational costs are subject to a known probability distribution. The model determines CCUS infrastructure plans to minimize the combination of total costs, environmental impact, and risk caused by uncertainties. The overall problem is a two-phase-two-stage stochastic multi-objective optimization problem, for which they present an algorithm for solving.

[Fuss, Szolgayova, Obersteiner and Gusti \(2008\)](#) employ a real options approach to study how policy and market uncertainties affect the decision-making of an electricity producer who is considering investing in CCS. While they do not address the CCUS infrastructure optimization problem, their work is relevant due to its incorporation of

policy uncertainty, specifically in the form of an unknown  $\text{CO}_2$  price. Their results show that policy uncertainty causes the decision-maker to delay investing in CCS technology in order to see whether the government will commit to further climate policy.

### 2.3 Novel contributions of this paper

This paper contributes to the branch of literature devoted to the CCUS infrastructure optimization problem in that we incorporate two novel features that were not present in the previous models. First, our model is formulated as a two-stage stochastic program to represent uncertain CCUS incentives in the second stage and optimal hedging decisions in the first stage. Second, we incorporate a risk-averse objective function that generalizes decision-making beyond the typical assumption of risk-neutral investment behavior. These novel model features enable us to answer our core research questions about the effects of policy uncertainty and risk aversion on CCUS investments. Lastly, our carefully parameterized case study of the Texas-Louisiana Gulf Coast sheds light on the relationship between CCUS policy incentives and deployment in a region with a high concentration of large  $\text{CO}_2$  point sources that is seen as a potential hub for CCUS development in the U.S.

## 3 Methodology

We develop two mixed-integer linear programs (MILPs) that dynamically invest in and operate CCUS infrastructure over multiple time periods in order to maximize profit. The model that will ultimately allow us to answer our research questions about the effects of policy uncertainty and risk aversion is a two-stage stochastic program. Before turning our attention to that model, we first present a deterministic MILP that we will use to obtain results for scenarios without policy uncertainty, which serve as benchmarks. By presenting the deterministic model first, we are able to clarify the model’s basic structure before shifting our focus to the extended features that distinguish the stochastic model. In our models, CCUS infrastructure consists of the following three components.

**Sources:** Sources are facilities that produce  $\text{CO}_2$ . They need to be opened (i.e., have  $\text{CO}_2$  capture equipment installed) before they can begin capturing  $\text{CO}_2$ . Once opened, they can capture up to some fixed maximum amount of  $\text{CO}_2$  per time period. These maximum amounts may vary with the particular source and the time period. There are several costs associated with sources: a fixed cost associated with opening a source, an operating and maintenance (O&M) cost per time period once a source is brought online, and a variable cost per ton of  $\text{CO}_2$  captured. All of these cost parameters may vary with time. For our case study we only consider large point sources of  $\text{CO}_2$ , which generally provide the most attractive capture opportunities.

**Sinks:** Sinks are locations where  $\text{CO}_2$  can be geologically stored or utilized in a production process. Like the sources, they must be opened (i.e., constructed/drilled) before they can begin storing  $\text{CO}_2$ . Furthermore, they have location- and time-dependent opening costs, O&M costs, and variable costs per unit of  $\text{CO}_2$  stored. Sinks each have

a known maximum cumulative storage capacity as well as a maximum injection rate (i.e., amount of CO<sub>2</sub> stored per time period). Additionally, a predetermined subset (possibly empty) of the sinks are CO<sub>2</sub> utilization sites where revenue can be earned for selling CO<sub>2</sub> to a customer with a positive willingness to pay for it – for example, an oil and gas producer engaged in EOR. This revenue is represented in the model as a negative variable cost.

**Pipelines:** Pipelines transport CO<sub>2</sub> between different locations in space. The pipelines have the same cost structure as the other infrastructure components, namely construction, O&M, and variable costs. Each pipeline segment connects two nodes and the segments are networked to enable complex flow patterns. Nodes can be sources, sinks, or junctions in the network. The pipelines move CO<sub>2</sub> from sources, potentially meet at junctions and merge/split, and then connect to sinks where CO<sub>2</sub> is deposited. The capacities of the pipelines are linked to their diameters and have investment costs that reflect economies of scale in their carrying capacities. In this study, we assume a small discrete set of possible pipeline diameters.

To incentivize the development and use of CCUS infrastructure, our models offer a reward for each ton of CO<sub>2</sub> that is captured, which appears as revenue in the objective function. The reward earned for each captured ton of CO<sub>2</sub> depends on whether it is injected into geologic storage or utilized, with the latter receiving a lower payout. These CCUS incentives are modeled directly on the 45Q tax credit in the U.S.

### 3.1 Deterministic model

Our deterministic model for CCUS infrastructure optimization is formulated in Eqs. (1)-(16), with the nomenclature defined in Table 1. Below, we explain the role of each equation in the formulation.

$$\begin{aligned}
\text{MAXIMIZE } \pi_1 = & \underbrace{\sum_{t \in \mathcal{T}} \sum_{j \in \mathcal{U}} C_{jt}^{\text{util}} b_{jt} (1 + \delta)^{-nt}}_{\text{Utilization Revenue}} + \underbrace{\sum_{t \in \mathcal{T}} \sum_{j \in \mathcal{U}} C_t^{\text{tax,u}} b_{jt} (1 + \delta)^{-nt} - \sum_{t \in \mathcal{T}} \sum_{j \in \mathcal{R}/\mathcal{U}} C_t^{\text{tax,g}} b_{jt} (1 + \delta)^{-nt}}_{\text{Tax Credit Revenue}} \\
& - \underbrace{\sum_{t \in \mathcal{T}} \sum_{i \in \mathcal{S}} (B_{it}^{\text{src}} \alpha_{it} + F_{it}^{\text{src}} s_{it} + V_{it}^{\text{src}} a_{it}) (1 + \delta)^{-nt}}_{\text{Capture Costs}} - \underbrace{\sum_{t \in \mathcal{T}} \sum_{r \in \mathcal{R}} (B_{rt}^{\text{res}} \beta_{rt} + F_{rt}^{\text{res}} r_{it} + V_{it}^{\text{res}} b_{it}) (1 + \delta)^{-nt}}_{\text{Storage Costs}} \\
& - \underbrace{\sum_{t \in \mathcal{T}} \sum_{(i,j) \in \mathcal{E}} \left( \left( \sum_{d \in \mathcal{D}} B_{ijdt}^{\text{p}} \gamma_{ijdt} + F_{ijdt}^{\text{p}} y_{ijdt} \right) + V_{ijt}^{\text{p}} z_{ijt} \right) (1 + \delta)^{-nt}}_{\text{Pipeline Costs}}
\end{aligned} \tag{1}$$

Subject to:

$$-\sum_{d \in \mathcal{D}} Q_{ijd}^p y_{ijdt} \leq x_{ijt} \leq \sum_{d \in \mathcal{D}} Q_{ijd}^p y_{ijdt} \quad \forall (i, j) \in \mathcal{E}, \quad \forall t \in \mathcal{T} \quad (2)$$

$$\sum_{j:(i,j) \in \mathcal{E}} x_{ijt} - \sum_{j:(j,i) \in \mathcal{E}} x_{jit} = \begin{cases} a_{it} & i \in \mathcal{S} \\ -b_{it} & i \in \mathcal{R} \\ 0 & \text{else} \end{cases} \quad \forall i \in \mathcal{N}, \quad \forall t \in \mathcal{T} \quad (3)$$

$$z_{ijt} \geq x_{ijt}, \quad z_{ijt} \geq -x_{ijt} \quad \forall (i, j) \in \mathcal{E} \quad \forall t \in \mathcal{T} \quad (4)$$

$$0 \leq a_{it} \leq R_i^{src} s_{it} \quad \forall i \in \mathcal{S}, \quad \forall t \in \mathcal{T} \quad (5)$$

$$0 \leq b_{jt} \leq R_j^{res} r_{jt} \quad \forall j \in \mathcal{R}, \quad \forall t \in \mathcal{T} \quad (6)$$

$$\sum_{t \in \mathcal{T}} b_{jt} \leq Q_j^{res} \quad \forall j \in \mathcal{R} \quad (7)$$

$$y_{ijdt} \geq y_{ijd(t-1)} \quad (i, j) \in \mathcal{E}, \quad \forall d \in \mathcal{D}, \quad \forall t \in \mathcal{T}/\{1\} \quad (8)$$

$$s_{it} \geq s_{i(t-1)} \quad \forall i \in \mathcal{S}, \quad \forall t \in \mathcal{T}/\{1\} \quad (9)$$

$$r_{jt} \geq r_{j(t-1)} \quad \forall j \in \mathcal{R}, \quad \forall t \in \mathcal{T}/\{1\} \quad (10)$$

$$\alpha_{it} = s_{it} - s_{i(t-1)} \quad \forall i \in \mathcal{S}, \quad \forall t \in \mathcal{T}/\{1\} \quad (11)$$

$$\beta_{jt} = r_{jt} - r_{j(t-1)} \quad \forall j \in \mathcal{R}, \quad \forall t \in \mathcal{T}/\{1\} \quad (12)$$

$$\gamma_{ijdt} = y_{ijdt} - y_{ijd(t-1)} \quad \forall (i, j) \in \mathcal{E}, \quad \forall d \in \mathcal{D}, \quad \forall t \in \mathcal{T}/\{1\} \quad (13)$$

$$a_{it}, b_{jt}, z_{ijt} \in \mathbb{R}_+ \quad (14)$$

$$x_{ijt} \in \mathbb{R} \quad (15)$$

$$y_{ijdt}, s_{it}, r_{jt}, \alpha_{it}, \beta_{jt}, \gamma_{ijdt} \in \{0, 1\} \quad (16)$$

The objective function (1) represents the profit to be maximized. It is defined as the revenues obtained from the 45Q incentives and from selling CO<sub>2</sub> to utilization sites, minus the costs of constructing, maintaining, and operating the CCUS infrastructure system.

The first few constraints model the flow of CO<sub>2</sub> through the network. Specifically, constraint (2) places bounds on the amount of CO<sub>2</sub> transported along edge  $(i, j)$  during time period  $t$ . Note that positive flow along  $(i, j)$  indicates that CO<sub>2</sub> flows from  $i \rightarrow j$ , whereas negative flow means that CO<sub>2</sub> flows from  $j \rightarrow i$ . If no pipeline exists along the edge, then its flow is constrained to be zero. If one or more pipelines exist along this edge, then the sum of the pipeline capacities serves as an upper bound on the flow of CO<sub>2</sub>. Constraint (3) states that the net flow out of each node must be balanced. Observe that the net flow can be positive, negative, or zero depending

Table 1: Model Nomenclature

Sets and Indices	
$\mathcal{N}$	The set of nodes in the network
$\mathcal{S} \subset \mathcal{N}$	The set of source nodes
$\mathcal{R} \subset \mathcal{N}$	The set of reservoir nodes
$\mathcal{U} \subset \mathcal{R}$	The set of utilization nodes
$\mathcal{D}$	The set of pipeline diameters
$\mathcal{T}$	The set of time periods
$\mathcal{E}$	The set of potential edges between nodes
$N_j \subset \mathcal{N}$	The set of nodes adjacent to node $j$
Decision Variables	
$x_{ijt}$	The amount of CO <sub>2</sub> transferred from node $i$ to node $j$ in period $t$
$z_{ijt}$	The absolute value of the amount of CO <sub>2</sub> transferred from node $i$ to node $j$ in period $t$
$y_{ijdt}$	Takes unit value if a pipeline of diameter $d$ exists between nodes $i$ and $j$ during period $t$
$a_{it}$	The amount of CO <sub>2</sub> captured by source $i$ during period $t$
$b_{jt}$	The amount of CO <sub>2</sub> stored in reservoir $j$ during period $t$
$s_{it}$	Takes unit value if source facility $i$ exists during period $t$
$r_{jt}$	Takes unit value if reservoir facility $j$ exists during period $t$
$\alpha_{it}$	Takes unit value if source facility $i$ is built during period $t$
$\beta_{jt}$	Takes unit value if reservoir facility $j$ is built during period $t$
$\gamma_{ijdt}$	Takes unit value if a pipeline of diameter $d$ is built between nodes $i$ and $j$ during period $t$
Parameters	
$B_{it}^{\text{src}}, B_{rt}^{\text{res}}, B_{ijdt}^{\text{p}}$	The investment costs for each infrastructure asset during period $t$
$F_{it}^{\text{src}}, F_{rt}^{\text{res}}, F_{ijdt}^{\text{p}}$	The O&M costs for each infrastructure asset during period $t$
$V_{it}^{\text{src}}, V_{rt}^{\text{res}}, V_{ijdt}^{\text{p}}$	The variable costs for each infrastructure asset during period $t$
$C_{jt}^{\text{util}}$	The revenue generated from selling one unit (ton) of CO <sub>2</sub> for utilization at node $j$ during period $t$
$C_t^{\text{tax,g}}$	The revenue generated from the tax credit for storing one unit (ton) of CO <sub>2</sub> using geologic storage during period $t$
$C_t^{\text{tax,u}}$	The revenue generated from the tax credit for storing one unit (ton) of CO <sub>2</sub> via EOR utilization during period $t$
$Q_{ijd}^{\text{p}}$	The max volume of CO <sub>2</sub> that can be moved along a pipeline of diameter $d$ between nodes $i$ and $j$
$R_i^{\text{src}}, R_i^{\text{res}}$	Maximum capture/storage rates for source $i$ /reservoir $j$ respectively
$Q_j^{\text{res}}$	Capacity of reservoir $j$
$\delta$	The discount rate
$n$	The number of years in each period

on the node type under consideration. Source nodes will have a non-negative net outflow and reservoir nodes will have a non-positive net outflow. Junction nodes, however, must have zero net outflow. We then have constraint (4), which sets the value of  $z_{ijt}$  to be the total flow along  $(i, j)$  during period  $t$ . We will need this value when we compute the variable costs of transporting CO<sub>2</sub>. Constraints (5) and (6) dictate that the rate at which CO<sub>2</sub> is captured/stored at a given facility is non-negative and bounded above by exogenous, facility-specific rates. If the relevant facility does not exist in a given time period, the amount that it captures/stores in that period is bound to be zero. Constraint (7) ensures that the total amount of CO<sub>2</sub> stored in a given reservoir over all time periods does not exceed the capacity of the reservoir.

The next group of constraints encodes the existence of infrastructure assets over all time periods after they are built and identifies the time periods when they are built (which allows us to properly account for construction costs, including discounting). Constraints (8), (9), and (10) ensure that once a piece of infrastructure is built, it continues to exist for the remaining time periods. Constraints (11), (12), and (13) are used to determine the time period (if any) in which each piece of infrastructure is built. The remainder of the constraints specify the domains of the variables.

## 3.2 Stochastic risk-averse model

With the foundational, deterministic model given, we now turn our attention to the two-stage stochastic programming model with a risk-averse objective. This model will allow us to address the primary research questions of our study: (1) To what extent does policy uncertainty diminish CCUS infrastructure investments? (2) How does the effect of policy uncertainty on CCUS investments depend on the degree of investor risk aversion?

The two-stage model divides the time periods into two decision-making stages. In the first stage, which is comprised of the first  $T$  time periods, the incentives for capturing CO<sub>2</sub> are known and the investor can construct infrastructure and capture CO<sub>2</sub>. These first-stage decisions are known as here-and-now decisions because they must be made at times when the incentive levels in the second stage are uncertain. In the second stage, the investor can continue to build and operate CCUS infrastructure subject to additional constraints: infrastructure that was built in the previous periods continues to exist, and the investor cannot exceed the remaining reservoir capacities. Furthermore, we assume that the incentive values that will be available in the second stage are unknown to the investor until the first stage ends and the second stage begins. However, we assume that the second-stage incentive levels will be drawn from a discrete probability distribution that is known to the investor in the first stage. Therefore, when making decisions about how much CCUS infrastructure to build in the first stage, the investor must hedge against the different possible realizations of the incentive levels in the second stage and their associated probabilities of occurring. For example, if there is a high probability of very low incentive levels in the second stage, then the investor may not be able to justify much CCUS infrastructure investment in the first stage, as investments may only pay off if more generous incentives persist for many years. On the other hand, if there is a high probability of lucrative incentives in the second stage, then the investor may want to avoid filling capacity-limited CO<sub>2</sub> reservoirs in the first stage in order to save their capacity for the future when the incentives will likely be more favorable. The two-stage model thus corresponds to the realistic situation in which policy incentives are known in the short run but are subject to considerable uncertainty in the long run, as they depend on the outcomes of political processes.

To incorporate risk aversion, we replace the profit maximization objective with an expected utility maximization objective, where the utility in each scenario is a quasiconcave function of the profit. Specifically, we assume that the investor has an isoelastic utility function  $u(w) = \frac{w^{1-\eta}}{1-\eta}$ , where  $w$  is total profit and  $\eta \geq 0$  is a risk parameter. A larger value of  $\eta$  reflects a more risk-averse investor, with  $\eta = 0$  designating risk-neutral investor behavior as a special case. Essentially, the isoelastic utility function gives us a simple way to define scenarios with different degrees of risk aversion by varying the value of  $\eta$ .

The expected utility maximization objective of the two-stage model is written as

$$\max_{\mathbf{x}} \mathbb{E} \left[ u \left( (\pi_1(\mathbf{x}) + z(\mathbf{x}, \tilde{\xi})) \right) \right],$$

where  $\mathbf{x}$  represents the feasible first-stage decisions,  $\pi_1$  denotes the first-stage profits, and  $z(\mathbf{x}, \tilde{\xi})$  is the second-stage

recourse problem with uncertain parameter  $\tilde{\xi}$ , which represent the 45Q incentive levels in the second stage. We assume that  $\tilde{\xi}$  is distributed according to a finite discrete probability distribution with  $|S|$  total realizations. In this case, scenario  $s \in S$  has 45Q incentive values  $\xi_s = (\xi_s^g, \xi_s^u)$  (the former value for geologic storage and the latter value for utilization), and occurs with probability  $p_s$ . Given that realization  $s$  occurs, the recourse problem is to maximize the profit obtained in the second stage,  $\pi_2(\mathbf{x}, \mathbf{y}_s, \xi_s)$ , by choosing recourse decisions  $\mathbf{y}_s$  subject to normal operating constraints and the constraints implied by the first-stage decisions  $\mathbf{x}$ . Given that scenario  $s \in S$  occurs, the overall profit is  $\pi_1(\mathbf{x}) + \pi_2(\mathbf{x}, \mathbf{y}_s, \xi_s)$ . Taking advantage of our discrete set of scenarios, we can now write our objective as

$$\max_{\mathbf{x}} \mathbb{E} \left[ u \left( \pi_1(\mathbf{x}) + z(\mathbf{x}, \tilde{\xi}) \right) \right] = \max_{\mathbf{x}, \mathbf{y}} \sum_{s \in S} p_s \cdot u \left( \pi_1(\mathbf{x}) + \pi_2(\mathbf{x}, \mathbf{y}_s, \xi_s) \right). \quad (17)$$

As written, Eq. (17) is a nonlinear objective function. Fortunately, we can linearize it using a piecewise linear approximation scheme. To do so, we first normalize the domain of our utility function to be  $[1, 2]$ , where 1 represents no profit and 2 is the maximum profit achievable under the most favorable 45Q scenario. With this normalization, we use  $L + 1$  equidistant points on  $[1, 2]$  to obtain  $L$  lines that piecewise approximate the utility function. Let the  $i$ -th line be denoted  $\ell_i(\cdot)$  and let the notation  $[L]$  denote the set  $\{1, 2, 3, \dots, L\}$ . We can then take advantage of the concavity of our objective function by introducing the variable  $\omega \in \mathbb{R}^s$  such that  $\omega_s \leq \ell_i \left( 1 + \frac{\pi_1(\mathbf{x}) + \pi_2(\mathbf{x}, \mathbf{y}_s, \xi_s)}{M} \right)$  for all  $i \in [L]$  and for each  $s \in [S]$ . Here,  $M$  is the normalization constant equal to the profit obtained in the most favorable scenario within  $S$ , which ensures that the realized profit will be on the domain  $[1, 2]$ . By introducing these additional linear constraints, we can simply write the (approximated) expected utility maximization objective as  $\max_{\omega} \sum_{s \in S} p_s \omega_s$ .

With these modeling assumptions, the full stochastic risk-averse model is presented in Eqs. (18)-(54). The model has many elements in common with the deterministic model and thus we mark second-stage decision variables with the ‘prime’ notation to make them easier to distinguish.

$$\text{MAXIMIZE } \sum_{s \in S} p_s \omega_s \quad (18)$$

Subject to:

$$\begin{aligned}
\pi_1 = & \underbrace{\sum_{t \in \mathcal{T}} \sum_{j \in \mathcal{U}} C_{jt}^{\text{util}} b_{jt} (1 + \delta)^{-nt}}_{\text{Utilization Revenue}} + \underbrace{\sum_{t \in \mathcal{T}} \sum_{j \in \mathcal{U}} C_t^{\text{tax,u}} b_{jt} (1 + \delta)^{-nt} - \sum_{t \in \mathcal{T}} \sum_{j \in \mathcal{R}/\mathcal{U}} C_t^{\text{tax,g}} b_{jt} (1 + \delta)^{-nt}}_{\text{Tax Credit Revenue}} \\
& - \underbrace{\sum_{t \in \mathcal{T}} \sum_{i \in \mathcal{S}} (B_{it}^{\text{src}} \alpha_{it} + F_{it}^{\text{src}} s_{it} + V_{it}^{\text{src}} a_{it}) (1 + \delta)^{-nt}}_{\text{Capture Costs}} - \underbrace{\sum_{t \in \mathcal{T}} \sum_{r \in \mathcal{R}} (B_{rt}^{\text{res}} \beta_{rt} + F_{rt}^{\text{res}} r_{it} + V_{it}^{\text{res}} b_{it}) (1 + \delta)^{-nt}}_{\text{Storage Costs}} \\
& - \underbrace{\sum_{t \in \mathcal{T}} \sum_{(i,j) \in \mathcal{E}} \left( \left( \sum_{d \in \mathcal{D}} B_{ijdt}^{\text{p}} \gamma_{ijdt} + F_{ijdt}^{\text{p}} y_{ijdt} \right) + V_{ijt}^{\text{p}} z_{ijt} \right) (1 + \delta)^{-nt}}_{\text{Pipeline Costs}}
\end{aligned} \tag{19}$$

$$\begin{aligned}
\pi_{2,s} = & \underbrace{\sum_{t \in \mathcal{T}_2} \sum_{j \in \mathcal{U}} C_{jt}^{\text{util}} b'_{jts} (1 + \delta)^{-nt}}_{\text{Second-Stage Utilization Revenue}} + \underbrace{\sum_{t \in \mathcal{T}_2} \sum_{j \in \mathcal{R}/\mathcal{U}} \xi_s^{gl} b'_{jts} (1 + \delta)^{-nt} - \sum_{t \in \mathcal{T}_2} \sum_{j \in \mathcal{U}} \xi_s^u b'_{jts} (1 + \delta)^{-nt}}_{\text{Second-Stage Tax Credit Revenue}} \\
& - \underbrace{\sum_{t \in \mathcal{T}_2} \sum_{i \in \mathcal{S}} (B_{it}^{\text{src}} \alpha'_{its} + F_{it}^{\text{src}} s'_{its} + V_{it}^{\text{src}} a'_{its}) (1 + \delta)^{-nt}}_{\text{Second-Stage Capture Costs}} - \underbrace{\sum_{t \in \mathcal{T}_2} \sum_{r \in \mathcal{R}} (B_{rt}^{\text{res}} \beta'_{rts} + F_{rt}^{\text{res}} r'_{its} + V_{it}^{\text{res}} b'_{its}) (1 + \delta)^{-nt}}_{\text{Second-Stage Storage Costs}} \\
& - \underbrace{\sum_{t \in \mathcal{T}_2} \sum_{(i,j) \in \mathcal{E}} \left( \left( \sum_{d \in \mathcal{D}} B_{ijdt}^{\text{p}} \gamma'_{ijdts} + F_{ijdt}^{\text{p}} y'_{ijdts} \right) + V_{ijt}^{\text{p}} z'_{ijts} \right) (1 + \delta)^{-nt}}_{\text{Second-Stage Pipeline Costs}} \quad \forall s \in [S]
\end{aligned} \tag{20}$$

$$\omega_s \leq \ell_i \left( 1 + \frac{\pi_1 + \pi_{2,s}}{M} \right) \quad \forall i \in [L], \quad \forall s \in [S] \tag{21}$$

$$- \sum_{d \in \mathcal{D}} Q_{ijd}^{\text{p}} y_{ijdt} \leq x_{ijt} \leq \sum_{d \in \mathcal{D}} Q_{ijd}^{\text{p}} y_{ijdt} \quad \forall (i,j) \in \mathcal{E}, \quad \forall t \in \mathcal{T} \tag{22}$$

$$\sum_{j:(i,j) \in \mathcal{E}} x_{ijt} - \sum_{j:(j,i) \in \mathcal{E}} x_{jit} = \begin{cases} a_{it} & i \in \mathcal{S} \\ -b_{it} & i \in \mathcal{R} \\ 0 & \text{else} \end{cases} \quad \forall i \in \mathcal{N}, \quad \forall t \in \mathcal{T}_1 \tag{23}$$

$$z_{ijt} \geq x_{ijt}, \quad z_{ijt} \geq -x_{ijt} \quad \forall (i,j) \in \mathcal{E} \quad \forall t \in \mathcal{T}_1 \tag{24}$$

$$0 \leq a_{it} \leq R_i^{\text{src}} s_{it} \quad \forall i \in \mathcal{S}, \quad \forall t \in \mathcal{T}_1 \tag{25}$$

$$0 \leq b_{jt} \leq R_j^{\text{res}} r_{it} \quad \forall j \in \mathcal{R}, \quad \forall t \in \mathcal{T}_1 \tag{26}$$

$$\sum_{t \in \mathcal{T}_1} b_{jt} \leq Q_j^{\text{res}} \quad \forall j \in \mathcal{R} \tag{27}$$

$$y_{ijdt} \geq y_{ijd(t-1)} \quad (i,j) \in \mathcal{E}, \quad \forall d \in \mathcal{D}, \quad \forall t \in \mathcal{T}_1/\{1\} \tag{28}$$

$$s_{it} \geq s_{i(t-1)} \quad \forall i \in \mathcal{S}, \quad \forall t \in \mathcal{T}_1/\{1\} \quad (29)$$

$$r_{jt} \geq r_{j(t-1)} \quad \forall j \in \mathcal{R}, \quad \forall t \in \mathcal{T}_1/\{1\} \quad (30)$$

$$\alpha_{it} = s_{it} - s_{i(t-1)} \quad \forall i \in \mathcal{S}, \quad \forall t \in \mathcal{T}_1/\{1\} \quad (31)$$

$$\beta_{jt} = r_{jt} - r_{j(t-1)} \quad \forall j \in \mathcal{R}, \quad \forall t \in \mathcal{T}_1/\{1\} \quad (32)$$

$$\gamma_{ijdt} = y_{ijdt} - y_{ijd(t-1)} \quad \forall (i, j) \in \mathcal{E}, \quad \forall d \in \mathcal{D}, \quad \forall t \in \mathcal{T}_1/\{1\} \quad a_{it}, b_{jt}, z_{ijt} \in \mathbb{R}_+ \quad (33)$$

$$x_{ijt} \in \mathbb{R} \quad (34)$$

$$y_{ijdt}, s_{it}, r_{jt}, \alpha_{it}, \beta_{jt}, \gamma_{ijdt} \in \{0, 1\} \quad (35)$$

$$-\sum_{d \in \mathcal{D}} Q_{ijd}^p y'_{ijdts} \leq x'_{ijts} \leq \sum_{d \in \mathcal{D}} Q_{ijd}^p y'_{ijdts} \quad \forall (i, j) \in \mathcal{E}, \quad \forall t \in \mathcal{T}_2, \quad \forall s \in [S] \quad (36)$$

$$z'_{ijts} \geq x'_{ijts}, \quad z_{ijts} \geq -x_{ijts} \quad \forall (i, j) \in \mathcal{E} \quad \forall t \in \mathcal{T}_2, \quad \forall s \in [S] \quad (37)$$

$$\sum_{j:(i,j) \in \mathcal{E}} x'_{ijts} - \sum_{j:(j,i) \in \mathcal{E}} x'_{jits} = \begin{cases} a'_{its} & i \in \mathcal{S} \\ -b'_{its} & i \in \mathcal{R} \\ 0 & \text{else} \end{cases} \quad \forall i \in \mathcal{N}, \quad \forall t \in \mathcal{T}_2, \quad \forall s \in [S] \quad (38)$$

$$0 \leq a'_{its} \leq R_i^{src} s'_{its} \quad \forall i \in \mathcal{S}, \quad \forall t \in \mathcal{T}_2, \quad \forall s \in [S] \quad (39)$$

$$0 \leq b'_{jts} \leq R_j^{res} r'_{jts} \quad \forall j \in \mathcal{R}, \quad \forall t \in \mathcal{T}_2, \quad \forall s \in [S] \quad (40)$$

$$\sum_{t \in \mathcal{T}_2} b'_{jts} \leq Q_j^{res} - \sum_{t \in \mathcal{T}_1} b_{jt} \quad \forall j \in \mathcal{R}, \quad \forall s \in [S] \quad (41)$$

$$y'_{ijdts} \geq y'_{ijd(t-1)s} \quad (i, j) \in \mathcal{E}, \quad \forall d \in \mathcal{D}, \quad \forall t \in \mathcal{T}_2, \quad \forall s \in [S] \quad (42)$$

$$s'_{its} \geq s'_{i(t-1)s} \quad \forall i \in \mathcal{S}, \quad \forall t \in \mathcal{T}_2, \quad \forall s \in [S] \quad (43)$$

$$r'_{jts} \geq r'_{j(t-1)s} \quad \forall j \in \mathcal{R}, \quad \forall t \in \mathcal{T}_2, \quad \forall s \in [S] \quad (44)$$

$$\alpha'_{its} = s'_{its} - s'_{i(t-1)s} \quad \forall i \in \mathcal{S}, \quad \forall t \in \mathcal{T}_2, \quad \forall s \in [S] \quad (45)$$

$$\beta'_{jts} = r'_{jts} - r'_{j(t-1)s} \quad \forall j \in \mathcal{R}, \quad \forall t \in \mathcal{T}_2, \quad \forall s \in [S] \quad (46)$$

$$\gamma'_{ijdts} = y'_{ijdts} - y'_{ijd(t-1)s} \quad \forall (i, j) \in \mathcal{E}, \quad \forall d \in \mathcal{D}, \quad \forall t \in \mathcal{T}_2, \quad \forall s \in [S] \quad (47)$$

$$y'_{ijd1s} \geq y_{ijd\mathcal{T}_1} \quad \forall (i, j) \in \mathcal{E}, \quad \forall d \in \mathcal{D}, \quad \forall s \in [S] \quad (48)$$

$$s'_{i1s} \geq s_{i\mathcal{T}_1} \quad \forall i \in \mathcal{S}, \quad \forall s \in [S] \quad (49)$$

$$r'_{j1s} \geq r_{j\mathcal{T}_1} \quad \forall j \in \mathcal{R}, \quad \forall s \in [S] \quad (50)$$

$$z'_{ijdts}, a'_{its}, b'_{jts} \in \mathbb{R}_+ \quad (51)$$

$$x'_{ijts}, \beta \in \mathbb{R} \quad (52)$$

$$y'_{ijdts}, s'_{its}, r'_{jts}, \alpha'_{its}, \beta'_{jts}, \gamma'_{ijdts} \in \{0, 1\} \quad (53)$$

$$\omega_s \in \mathbb{R} \quad \forall s \in [S] \quad (54)$$

Constraint (19) defines the profit obtained during the first stage. Similarly, in constraint (20), we define the profit earned in the second stage under each realization of the future incentive levels. With these profit components defined, we can concisely write constraint (21) to ensure that the utility in each scenario is tight to the piecewise linear approximation of the true, nonlinear utility function. Constraints (22)-(35) follow the same logic as in the deterministic model and are applied to the first-stage decision variables. Similarly, constraints (36)-(54) are the second-stage constraints and follow the same logic as the first-stage constraints, with a few notable exceptions.

Constraint (41) ensures that in every scenario the volume of CO<sub>2</sub> stored at each sink in the second stage does not exceed the remaining capacity after the first stage. To ensure that infrastructure built in the first stage continues to exist at the start of the second stage, we have constraints (48), (49) and (50). The remainder of the constraints specify the domains of the new variables.

### 3.3 Pipeline network generation

To run the presented models, we need to define sets of potential CO<sub>2</sub> sources, sinks, and pipelines. While the sources and sinks can be chosen from available databases, the potential network of pipelines that could be built to connect them is harder to establish. To obtain a network of potential pipelines, we implement a candidate network generation algorithm that is similar to the one presented by [Middleton and Bielicki \(2009\)](#). We first select our sets of potential sources and sinks. Then, we place a bounding rectangular grid of resolution 300m × 300m over the selected sets. We give each cell in the grid a unit value. Next, we use different land-use multipliers to obtain the cost of building a pipeline across that cell. These multipliers take into account factors such as slope, urban density, railroad crossings, topography, and so on. Once the cost of each cell is calculated, we run a least-cost path algorithm that matches each source to each sink and merges the resulting paths into one large network. The resulting network typically has many overlapping paths, so we combine coincident or nearby paths to reduce complexity. Lastly, we place junction nodes at the points of intersection in the network and partition the network into arcs with the nodes as endpoints. Each arc has a construction cost given by the sum of multipliers over the cells it passes through, multiplied by the base cost of building a pipeline of minimum diameter (10 inches in our case study) over 300m. This candidate pipeline generation algorithm is implemented in ArcGIS Pro.

### 3.4 Texas-Louisiana Gulf Coast case study parameterization

To study the effects of policy uncertainty and risk aversion on CCUS infrastructure development, we analyze a case study of the Texas-Louisiana Gulf Coast region. This region is chosen due to its high concentration of large CO<sub>2</sub>-producing facilities, abundance of geological formations that are suitable for CO<sub>2</sub> storage, and numerous oil and gas fields that provide ample opportunities for CO<sub>2</sub> utilization for EOR. As for the general assumptions of the case study, we represent three time periods lasting ten years each. The first period belongs to the first decision-making stage while the second and third periods are part of the second decision-making stage. We assume a discount rate

of 7%. We now describe how we parameterize the sets of candidate sources, sinks, and pipelines, then outline the 45Q incentive level distributions and risk aversion settings that we consider.

### 3.4.1 Sources

We select CO<sub>2</sub> sources to include in our case study from the EPA Flight Database, which contains detailed information about thousands of CO<sub>2</sub>-emitting facilities including the type of facility, geographic location, and annual carbon output (EPA, 2022). The annual carbon output and the facility type are used in conjunction with cost estimates from the National Petroleum Council (2019) to parameterize the costs of building and operating a CO<sub>2</sub> capture unit at each facility. The values are scaled according to the relative CO<sub>2</sub> output of each facility and its type. The set of potential sources in our case study is reported in Table 2, with the source locations depicted visually as the red nodes on the map in Figure 1.

Table 2: Potential CO<sub>2</sub> sources included in the Texas-Louisiana Gulf Coast case study.

Facility Name	Address	City	County	State	Parent Companies	Output (T/Yr)	Type
ExxonMobil Bt Site	5000 Bayway Dr	Baytown	Harris County	TX	Exxon M Corp	11,076,876	Refineries
W A Parish	Yu Jones Rd	Thompsons	Fort Bend	TX	Nrg Energy Inc	10,433,780	Power Plant
Motiva Enterprises Llc	2555 Savannah Ave	Port Arthur	Jefferson County	TX	Aramco Services Co	4,869,641	Refineries
Dow Texas Operations Freeport	2301 N. Brazosport Blvd.	Freeport	Brazoria County	TX	Dow Inc	4,535,617	Chemical
Sabine Pass Lng Terminal	9243 Gulf Beach Hwy	Johnsons Bayou	Cameron Parish	LA	Cheniere Energy Inc	4,097,366	Petroleum & Natural Gas
Deer Park Energy Center	5665 Highway 225	Deer Park	Harris	TX	Volt Parent Lp	4,041,179	Power Plant
Galveston Bay Refinery	2401 5th Ave S In Texas City	Texas City	Galveston County	TX	Marathon Petroleum	3,903,627	Refineries
ExxonMobil Beaumont Refinery	1795 Burt St	Beaumont	Jefferson	TX	Exxon Mobil Corp	3,883,442	Refineries
Cameron Lng. Llc	301 N. Main Street	Hackberry	Cameron Parish	LA	Sempra Energy	3,320,589	Petroleum & Natural Gas
Citgo Petroleum Corp	4401 Hwy 108	Westlake	Calcasieu Parish	LA	Pdv America Inc	3,312,402	Refineries
Sweeny Cogeneration Facility	7190 Old Fm 524, Gate 13	Old Ocean	Brazoria County	TX	Phillips 66 (100%)	3,310,561	Power Plant
Channelview Cogeneration Facility	8580 Sheldon Road	Houston	Harris	TX	Eif Channelview Llc	2,854,833	Power Plant
Sabine	West Roundbunch Road	Bridge City	Orange	TX	Entergy Corp	2,716,827	Power Plant

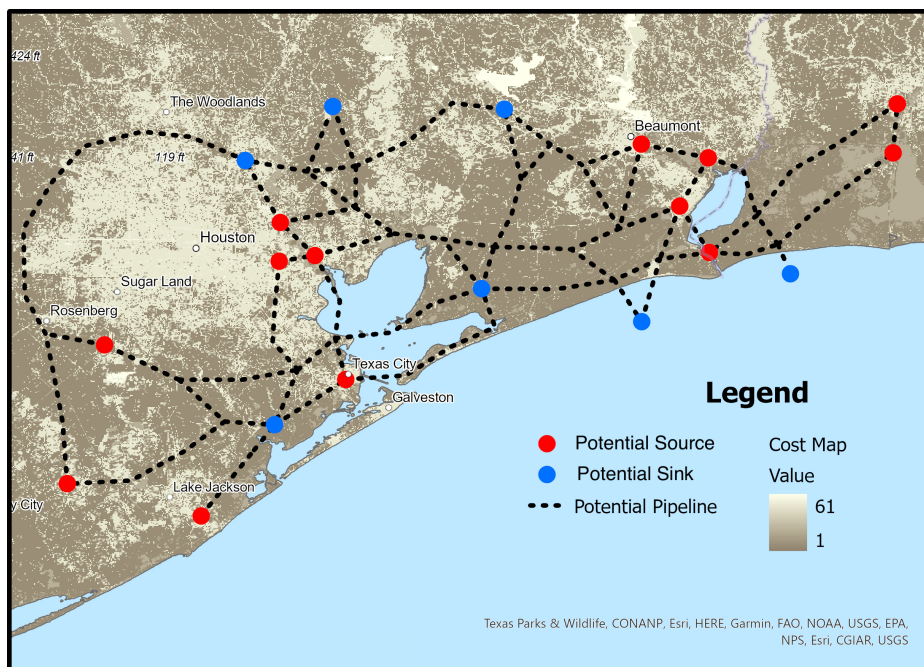


Figure 1: Potential CO<sub>2</sub> sources, sinks, and pipelines included in the Texas-Louisiana Gulf Coast case study.

### 3.4.2 Sinks

The Texas-Louisiana Gulf Coast region has an abundance of potential CO<sub>2</sub> storage locations. In our case study, we consider only two types of storage locations: saline aquifers (for geologic storage) and active oil and gas fields (for utilization for EOR). While storage sites are spread throughout the region, we aggregate them at several discrete locations and parameterize their capacities based on data from the [National Energy Technology Laboratory \(2015\)](#). The maximum injection rates are parameterized with data from [Carneiro, Martinez, Suárez, Zarhloule and Rimi \(2015\)](#) and the capital, O&M, and variable costs are parameterized using data from the [International Energy Agency \(2011\)](#) and the [National Petroleum Council \(2019\)](#). Additionally, the price that oil and gas producers pay for CO<sub>2</sub> that they will use for EOR is set to \$40 per ton in accordance with an estimate from [Middleton \(2013\)](#). The potential sinks (both geologic storage and utilization) included in our case study appear in Figure 1 as the blue nodes on the map.

### 3.4.3 Pipelines

With our source and sink locations chosen, we generate a candidate pipeline network using the algorithm described in Section 3.3. For our case study, we include three distinct pipeline diameters (10in, 20in, and 30in) that the investor can build along each arc, with their respective capacities calculated based on [Smith \(2021\)](#). The capital, O&M, and variable costs are established using data from [Tutton \(2018\)](#) and the [National Petroleum Council \(2019\)](#) for each pipeline diameter and arc length. The candidate pipeline network is depicted on the map in Figure 1 as dashed black lines.

### 3.4.4 Incentive levels, probability distributions, and risk aversion

We consider five possible realizations for the 45Q incentive levels in the second stage, which are (in \$/tonCO<sub>2</sub> with the geologic storage level written first, then the utilization level): (0,0), (42.5,30), (85,60), (127.5,90), and (170,120). The central (85,60) incentive levels represent a continuation of the first-stage incentive levels, as established by the Inflation Reduction Act, through the second stage. The (0,0) scenario represents the elimination of CCUS incentives by the government in the future, while the (42.5,30) scenario reduces the incentives to half of their current levels. The more favorable (127.5,90) and (170,120) scenarios increase the incentives to 50% and 100% more than their current levels, respectively.

To generate useful benchmark results, we first solve the deterministic model for all five realizations of the future 45Q incentive levels, assuming perfect information about what they will be. Then, we run the stochastic risk-averse model with five different discrete probability distributions over the possible second-stage incentive levels. These five probability mass functions (PMFs) – Uniform, Small Peak, Medium Peak, Large Peak, and Spike – are shown graphically in Figure 2. It is important to note that all of the distributions have the same mean but different variances, and thus reflect different amounts of uncertainty regarding future incentives for CCUS. The Uniform

distribution assumes the most uncertainty about the future policy environment because all of the realizations are equally likely to occur. The Spike distribution assumes the least uncertainty because the current incentive levels are very likely to remain in place.

For each probability distribution over future 45Q incentive levels, we solve the stochastic risk-averse model with different values of  $\eta$  to investigate the effects of varying degrees of risk aversion. Specifically, we obtain results for  $\eta$  values between 0 (the risk-neutral case) and 7 (a highly risk-averse case).

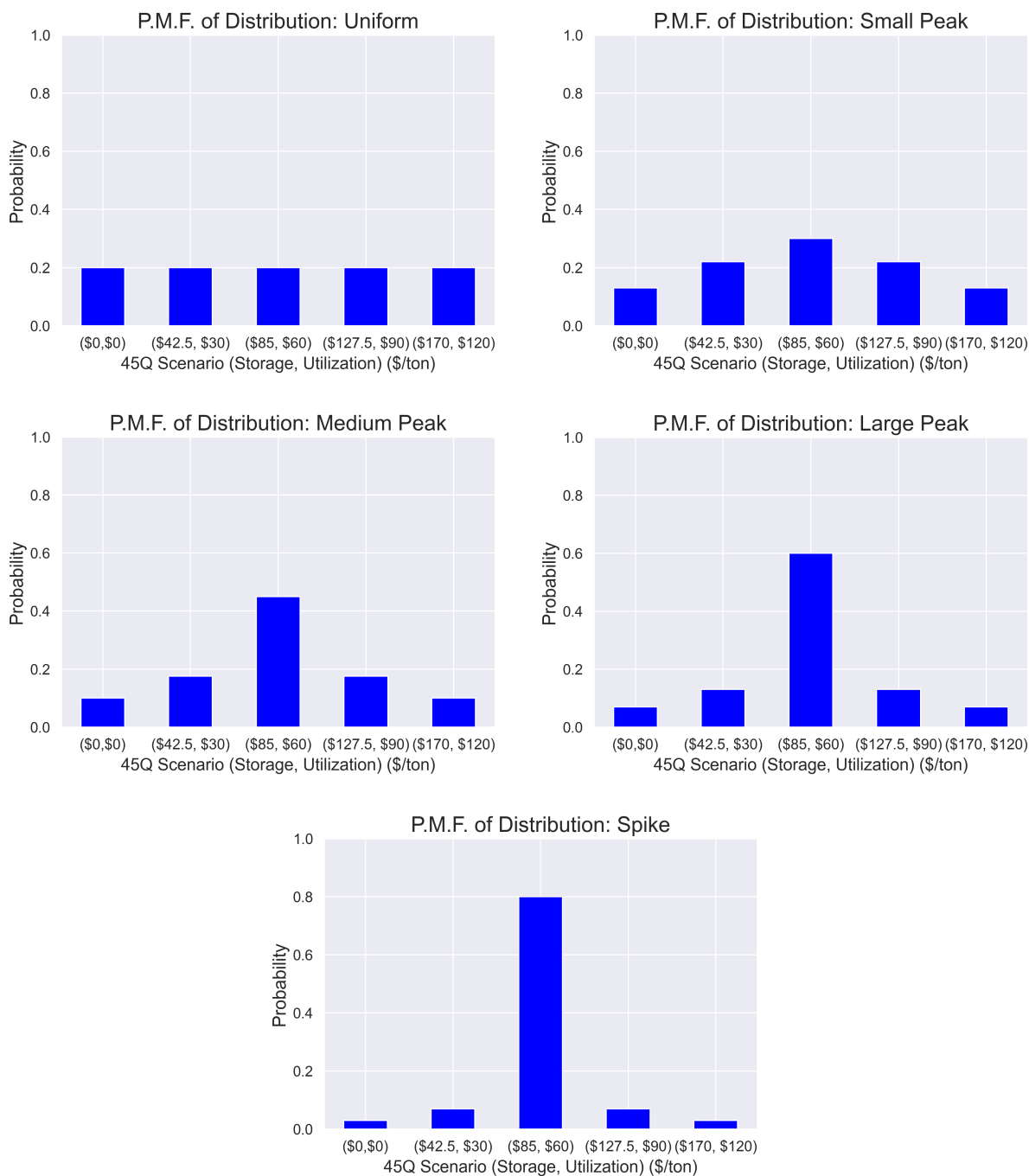


Figure 2: Probability distributions over the possible second-stage 45Q incentive levels.

## 4 Results and discussion

### 4.1 Deterministic model results

While the deterministic model’s assumption of perfect foresight of future incentive levels is unrealistic, the deterministic solutions provide useful benchmarks against which we can compare the solutions we will obtain from the stochastic risk-averse model. In each deterministic model run, we assume that the current 45Q incentive levels hold for the first ten-year period (the first stage) and then one of the five possible incentive level realizations applies in the next two periods (the second stage). At a high level, the results of these deterministic model runs are summarized in Figures 3 and 4. The former shows the total amount of CO<sub>2</sub> captured over the 30-year timeframe and the latter reveals the total investment in CCUS infrastructure, broken down into capture, transportation, and storage assets.

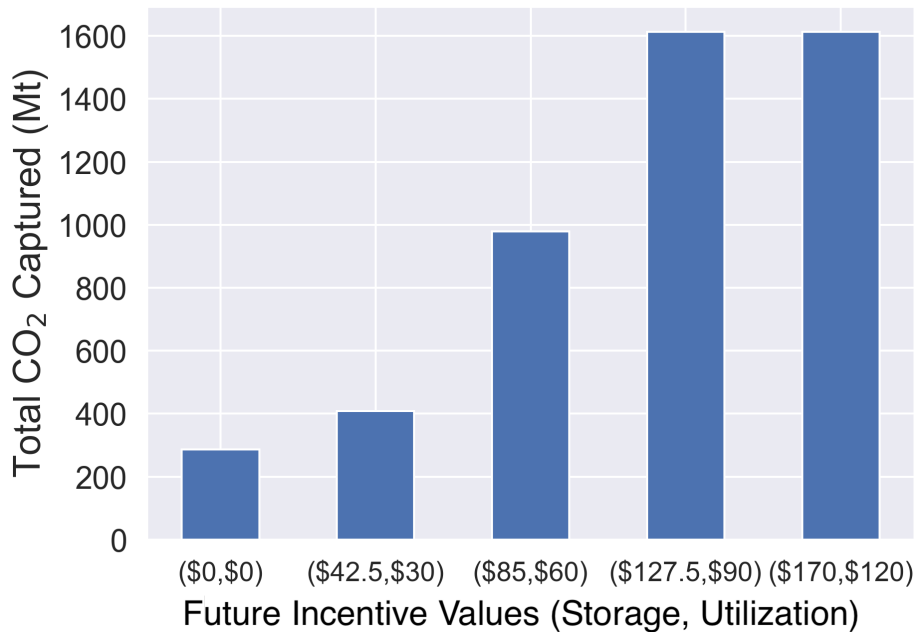


Figure 3: Total CO<sub>2</sub> captured over 30 years for each scenario of future incentive levels in the deterministic model.

As expected, we see that as the values of the incentives increase, total CCUS infrastructure investment and total CO<sub>2</sub> captured both rise as more CCUS projects become profitable. These trends continue until the transition from the (\$127.5, \$90) levels to the (\$170, \$120) levels does not induce further increases in CCUS deployment, since the former are already sufficient to make all CO<sub>2</sub> capture facility investments profitable. Several scenarios are worth commenting on individually. If the future 45Q values remain at their current levels of (\$85, \$60), then the optimal solution includes roughly \$23 billion of CCUS investments over the next 30 years. Interestingly, even if the incentive values were to decrease by a factor of two for the final two decades (dropping to (\$45.5, \$30) per ton of CO<sub>2</sub>), CCUS investments would be nearly the same but the total amount of CO<sub>2</sub> captured would decrease significantly. This is because, as the incentives increase, the infrastructure planner can afford to develop infrastructure components that

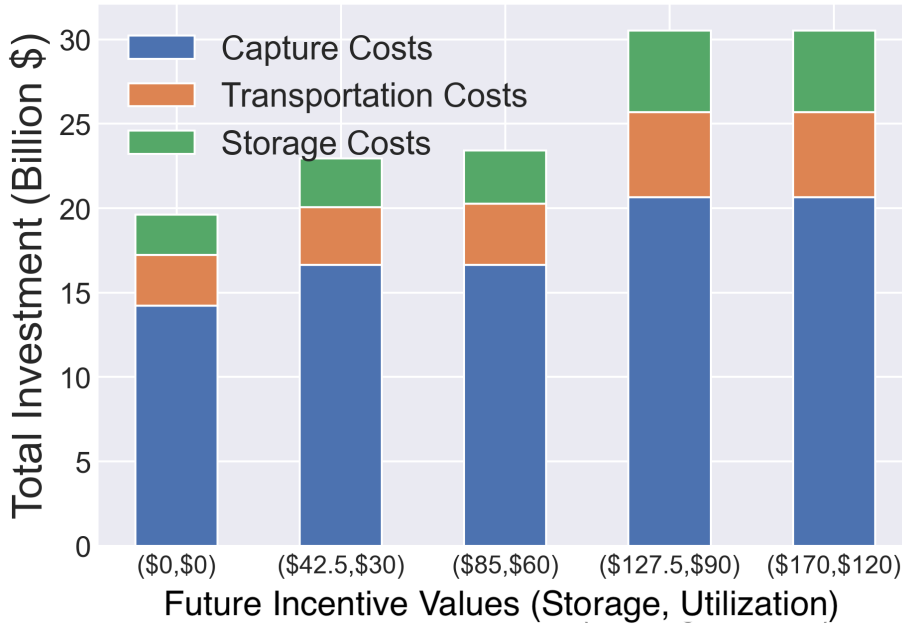


Figure 4: Total CCUS infrastructure investment for each scenario of future incentive levels in the deterministic model.

better leverage economies of scale through a more connected pipeline network and/or more cost-efficient sources and sinks. Also notable are the CCUS investments in the scenario where there are no second-stage incentives. Nearly \$20 billion of CCUS investments are justified, resulting in about 300 Mt of captured CO<sub>2</sub>, even if the 45Q incentives were to disappear after the first ten years. This implies that with the current incentive levels of (\$85, \$60), a fair number of CCUS projects should be profitable with a payback period of less than a decade.

Figures 5-8 present map-based visualizations of the optimal CCUS infrastructure network in each deterministic scenario at the end of the 30-year timeframe. They distinguish assets that are built in the first stage (first decade) from assets that are built in the second stage (second and third decades), to facilitate comparisons with the two-stage stochastic programming results. Note that in Figures 5, 6, and 7, representing the cases with future incentive levels of (\$0, \$0), (\$42.5, \$30) and (\$85, \$60) per ton respectively, we see similar infrastructure investments in the first stage and no additional infrastructure being developed in the second stage. As mentioned in the previous paragraph, the infrastructure built in Figure 5 is profitable solely on the basis of the current incentive levels being available for the first ten years (since the second-stage incentives in this scenario are zero). Although similar to the previous figure, in Figure 6, we see a larger diameter pipeline built to move larger quantities of CO<sub>2</sub> to take advantage of the higher second-stage incentives. When the second-stage incentives match the current values of (\$85, \$60), depicted in Figure 7, we see the pipeline network become more connected to better leverage economies of scale.

We now turn our attention to the deterministic scenario results with second-stage incentives of (\$127.5, \$90) and

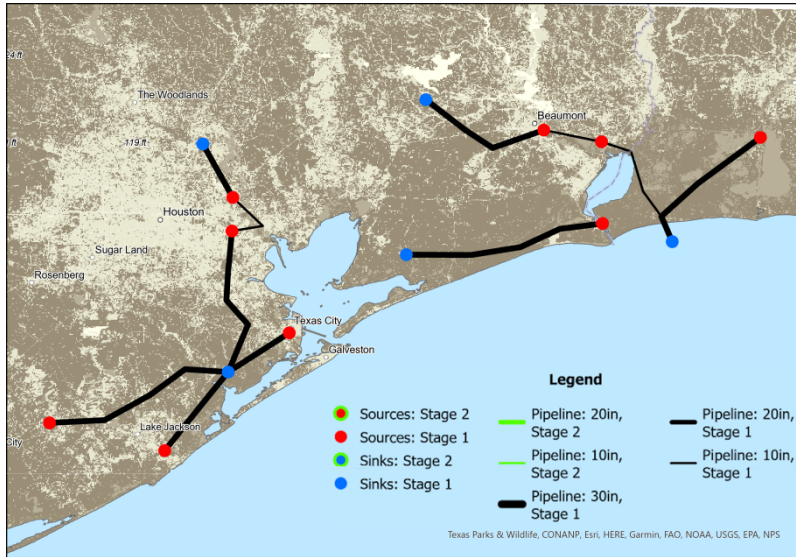


Figure 5: Optimal infrastructure investments for the deterministic scenario with future incentives (\$0, \$0).

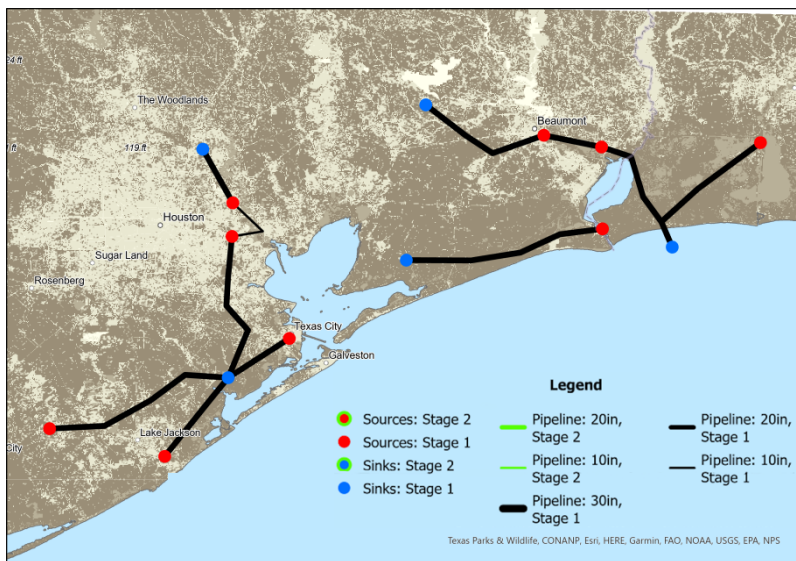


Figure 6: Optimal infrastructure investments for the deterministic scenario with future incentives (\$42.5, \$30).

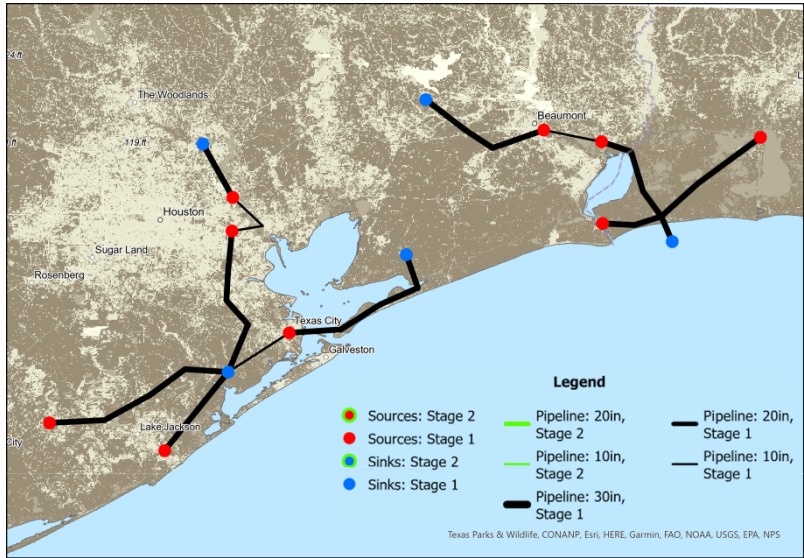


Figure 7: Optimal infrastructure investments for the deterministic scenario with future incentives (\$85, \$60).

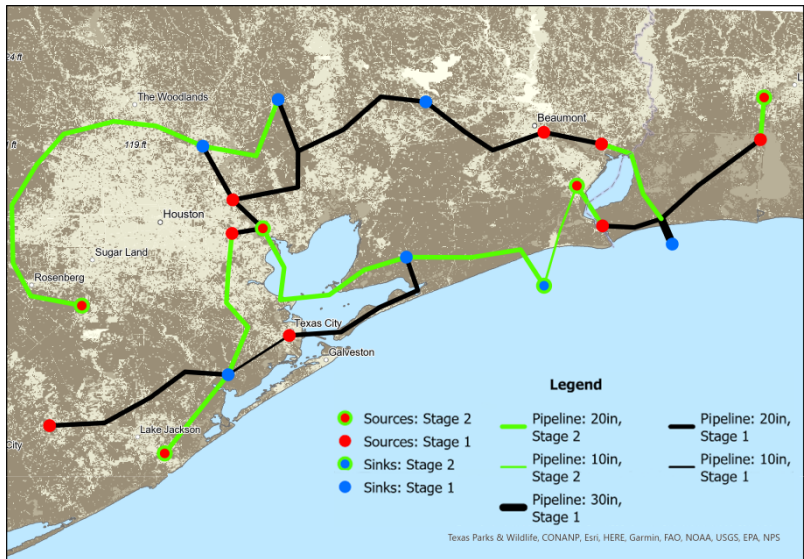


Figure 8: Optimal infrastructure investments for the deterministic scenarios with future incentives (\$127.5, \$90) and (\$170, \$120), as they are the same.

(\$170, \$120). Their optimal investments are the same and displayed in Figure 8. With these future increases in 45Q values, we not only observe a difference in first-stage infrastructure investments but also see additional second-stage infrastructure development. In the second stage, more CO<sub>2</sub> capture facilities are added to exploit the more generous incentives. Sources that were prohibitively costly under the current incentive values become profitable to open and pipelines are built to connect them to the network. These CCUS assets are not built in the first stage because they would accrue unnecessary O&M costs, so it is better to delay their construction until the second stage.

From these deterministic scenarios, we see that total CCUS infrastructure investment and total CO<sub>2</sub> captured can vary greatly depending on the future values of the 45Q incentives. As the incentive values increase, the amounts of CCUS investment and CO<sub>2</sub> capture increase as well. Higher future incentive levels make more facilities profitable and allow the investor to take advantage of economies of scale with a larger and more connected pipeline network. At some point, these effects saturate and higher incentives will not promote additional CO<sub>2</sub> capture, as the network will hit its maximum CO<sub>2</sub> capture capacity. Lastly, we find that the current 45Q levels are sufficient to drive near-term CCUS development regardless of future incentive values and justify roughly 300 Mt of CO<sub>2</sub> capture in the next decade. These deterministic model results will serve as baselines against which we will compare the results with policy uncertainty and risk aversion in the next subsection.

## 4.2 Results with policy uncertainty and risk aversion

We run our two-stage model using each of the five probability distributions over future incentive levels from Figure 2 and risk aversion settings of  $\eta = 0, 0.5, 1.5, 3, \text{ and } 7$ . Recall that  $\eta = 0$  is the risk-neutral case while  $\eta = 7$  is an extremely risk-averse case. For these experiments, we are particularly interested in the near-term CCUS investments in the first stage when the future policy is uncertain. By contrast, the second-stage investments will depend on the realized second-stage incentive levels. The optimal first-stage infrastructure investments are shown in Figure 9. From the figure, we see several notable results. First, we note that the minimum investment level for any risk aversion setting and incentive distribution is slightly less than \$20 billion. This minimum investment level is consistent with the total first-stage investments in the deterministic scenario with future 45Q values of (\$0, \$0), which appeared in Figure 4. This reinforces our finding that there is a baseline level of investment justified by the current 45Q incentives even if they are only available for the next decade before being eliminated.

Next, we observe that as the distribution of future incentive values becomes less uncertain, moving from the Uniform to the Spike distribution, the total amount of first-stage investment increases to roughly \$23 billion. This investment level is consistent with the amount invested in the deterministic scenario with second-stage incentives of (\$85, \$60), whose results were seen in Figure 4. This finding matches our intuition. Each of our future incentive distributions has mean incentives of (\$85, \$60), so as their probability mass becomes more concentrated about their mean, we would expect the infrastructure decisions made to approach those of the deterministic scenario with second-stage incentives of (\$85, \$60), which included approximately \$23 billion of first-stage investments. For the

remainder of this paper, we will refer to the results of the deterministic model with second-stage incentives (\$85, \$60) as the “deterministic baseline.”

When we examine first-stage investment with respect to the risk aversion setting, we see that as the investor becomes more risk-averse, the amount of first-stage investment tends to increase. At first glance, this may seem counterintuitive. However, by examining the CO<sub>2</sub> captured in the first stage, we are able to gain some intuition into why this is happening. Figure 10 shows the expected total CO<sub>2</sub> captured over the 30-year timeframe (left panel) and only the CO<sub>2</sub> captured in the first stage (right panel). Its right panel reveals that low levels of risk aversion are associated with lower first-stage CO<sub>2</sub> capture levels than the deterministic baseline. However, as risk aversion increases we see the first-stage CO<sub>2</sub> capture for every distribution converge to that of the deterministic baseline. This is because a less risk-averse investor is willing to capture less CO<sub>2</sub> in the first stage in order to preserve reservoir capacity for the second stage, when the investor hopes that the incentives will be more lucrative. On the other hand, a more risk-averse investor would rather capture more CO<sub>2</sub> in the first stage when the 45Q levels are known with certainty, instead of preserving reservoir capacity for the uncertain future policy. With a higher degree of risk aversion and intertemporal capacity constraints for the most attractive CO<sub>2</sub> sinks, the certain present is a more appealing time to inject CO<sub>2</sub> into geologic storage than the uncertain future.

We find that there is an ambiguous relationship between risk aversion and expected CO<sub>2</sub> captured over the 30-year timeframe, results that appear in the left panel of Figure 10. Nevertheless, we can make several observations. Looking at Figure 10, we see that the expected amount of CO<sub>2</sub> captured, regardless of risk aversion level, is bounded from above by the CO<sub>2</sub> captured in the deterministic baseline. This is sensible; introducing policy uncertainty and/or risk aversion does not cause expected CO<sub>2</sub> capture to increase. On the more risk-averse end of the spectrum, we see that for the Spike distribution that has the least uncertainty, the model converges to capture the same amount of CO<sub>2</sub> in expectation as in the deterministic baseline. This aligns with our intuition since the Spike distribution is closest in distribution to the deterministic scenario with the (\$85, \$60) incentive values. In addition, at the highest risk aversion level of  $\eta = 7$ , we see that the expected CO<sub>2</sub> captured is decreasing in the amount of uncertainty reflected in the incentive level distributions, as the lines are in order from the Uniform distribution at the bottom to the Spike distribution at the top. With significant risk aversion, policy uncertainty reduces the expected amount of CO<sub>2</sub> capture.

It should be noted that regardless of the future incentive level distribution and risk aversion setting, the combined effect of the two leads to at most a 7% reduction in expected total CO<sub>2</sub> captured over the time horizon in all experiments. This suggests that policy uncertainty and risk aversion may have limited impacts on CCUS development when the current incentives are sufficient to justify considerable investment, as we have seen is the case with the current 45Q policy.

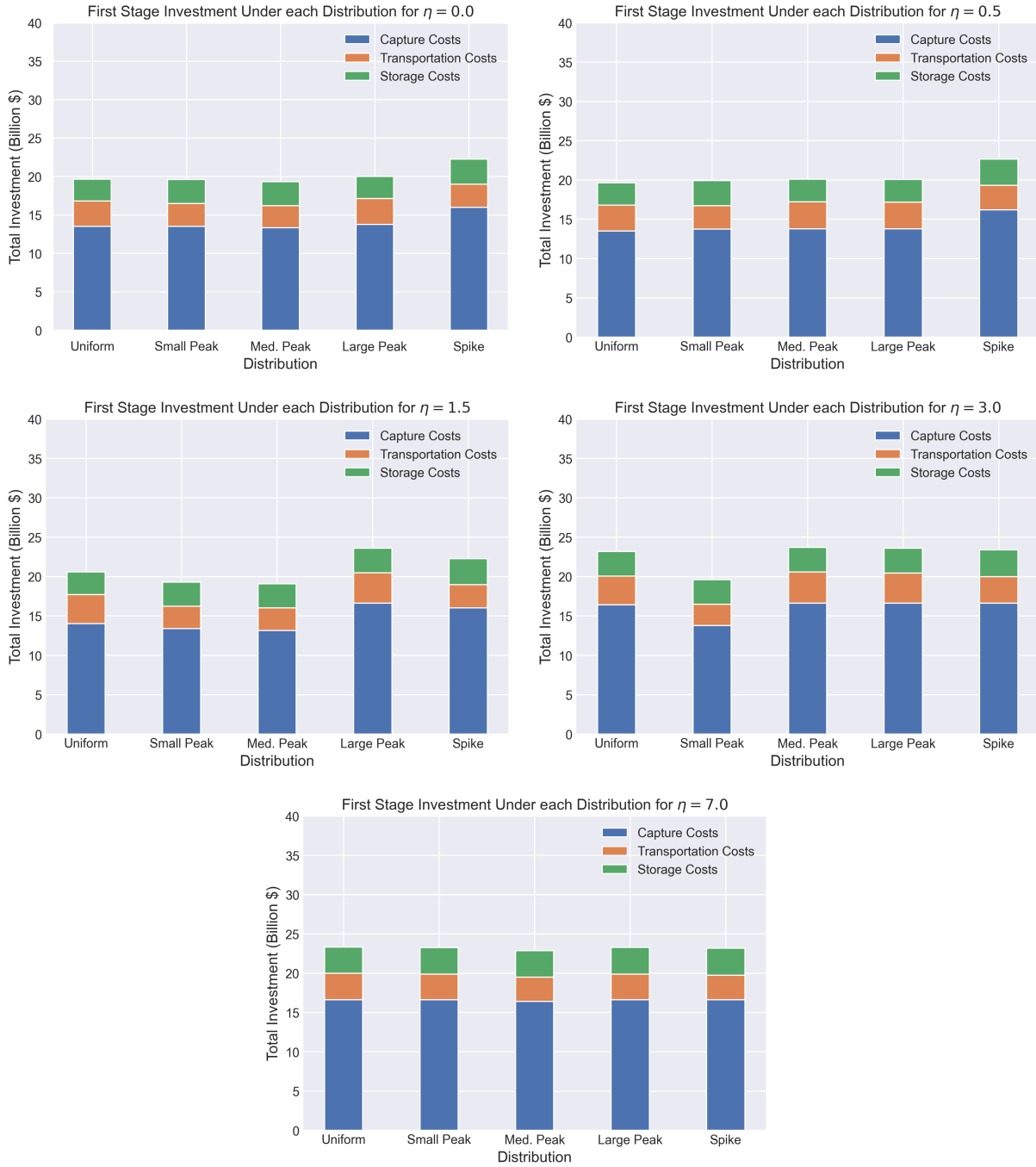


Figure 9: Optimal first-stage investments with each incentive level distribution (columns) and risk aversion setting (panels) for the two-stage model.

## 5 Conclusions and policy implications

Our primary research questions were: (1) To what extent does policy uncertainty diminish CCUS infrastructure investments? (2) How does the effect of policy uncertainty on CCUS investments depend on the degree of investor risk aversion? To answer these questions, we developed two closely related optimization models for CCUS infrastructure development. One was a deterministic model, whereas the other was a two-stage stochastic program with

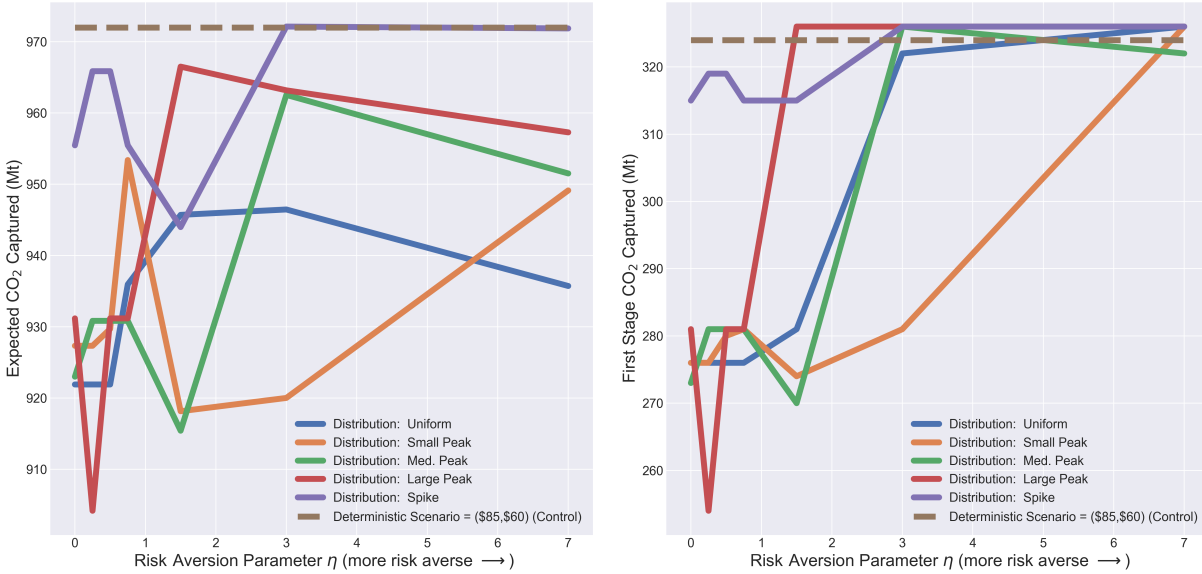


Figure 10: Expected CO<sub>2</sub> captured over the 30-year timeframe (left) and only in the first stage (right) for each combination of incentive level distribution (lines) and risk aversion setting (horizontal axes).

policy uncertainty and risk aversion, model features that are new to the literature on CCUS infrastructure network optimization. We applied both of the models to an empirically parameterized case study of the Texas-Louisiana Gulf Coast region.

The main findings from our case study can be summarized as follows:

- The current 45Q incentive levels in the United States ought to be sufficient to drive meaningful CCUS infrastructure investment for the next decade, regardless of future policy uncertainty or investor risk aversion.
- Policy uncertainty and risk aversion lead to at most a 7% decline in expected CO<sub>2</sub> captured over the next 30 years, relative to the deterministic case in which the current incentives levels persist.
- Risk aversion has an ambiguous effect on the amount of CO<sub>2</sub> captured. A less risk-averse investor may actually undertake less CCUS infrastructure investment and CO<sub>2</sub> capture in the near term in order to preserve sink capacity for the future, in case the incentives become more lucrative.

Our findings have several notable implications for policymakers seeking to accelerate the deployment of CCUS technologies. First, the availability of the 45Q tax credits at their current levels for one decade should be sufficient to induce considerable CCUS investment in the U.S. Second, as seen in our deterministic results for total CO<sub>2</sub> captured in Figure 3, raising the incentive levels by 50% would lead to significantly more CO<sub>2</sub> capture. Beyond those levels, making the incentives even more generous may not result in much additional CO<sub>2</sub> capture since suitable projects would already have become profitable at lower incentive levels. Third, even though policy uncertainty and risk aversion have a limited impact on expected total CO<sub>2</sub> capture in our scenarios (at most a 7% effect), reducing policy uncertainty would help avoid this reduction in CCUS activity. Certainly, policymakers must balance the

advantages of credible, long-term policy commitments against the benefits of maintaining flexibility to adjust policies as new information comes to light. One appealing compromise could be to place floors, and perhaps ceilings as well, on the future values of the 45Q tax credit levels, similar to CO<sub>2</sub> emissions trading systems that incorporate a price floor. This approach would reduce policy uncertainty without committing to a single long-term trajectory of incentive levels. Fourth, our results have shown how investor risk aversion may not actually cause delays in CCUS investments, since a more risk-averse investor may want to maximally exploit the current, known incentives instead of preserving CO<sub>2</sub> storage capacity for unknown, future incentives. Therefore, we do not find evidence to indicate that investor risk aversion is a major impediment to CCUS development.

Our study entailed several limitations that should be kept in mind when interpreting its results and could be addressed in future work. First, the size of our case study was limited by the computational complexity of solving our MILPs. We believe that a larger case study would be more representative of the Texas-Louisiana Gulf Coast region, which has abundant CO<sub>2</sub> sources and sinks. In particular, with more storage locations, a less risk-averse investor may not have as much incentive to preserve sink capacity for the second stage, as storage limitations are less likely to serve as binding constraints on the optimal solution. To experiment with larger case studies without encountering excessive solution times, we could reduce the number of integer variables in the models, which presents its own downsides. Second, the data used to parameterize our case study came from a wide variety of publicly available sources and was pieced together into a cohesive case study to the best of our abilities. We recognize that some of the parameter values, especially the cost assumptions, may not be entirely accurate descriptions of the true values of these parameters in the real world. Future work could benefit greatly from additional data on CCUS costs and other parameters. In the meantime, researchers could do additional sensitivity and scenario analyses with varying assumptions or even treat these parameters as uncertain, as we did for future policy incentives.

There are several future research questions that could be examined using the models that we have developed. An interesting and straightforward extension would be to consider a wider range of future 45Q distributions. In this study, we only considered distributions that were symmetric about the current incentive levels in order to isolate the effects of policy uncertainty. However, we could imagine more “pessimistic” distributions that are weighted more toward low and zero incentive levels and investigate whether policy uncertainty and risk aversion have fundamentally different implications in this context. It is notable that while we were carrying out this study, the 45Q values were changed from (\$50, \$35) to their current values of (\$85, \$60). Assuming that the current incentives are available for the next ten years, we found that considerable CCUS investment is justified even if the policy will be eliminated afterward. It would be interesting to run our experiments with policy uncertainty and risk aversion but with less generous incentives in the near term. In this case, the effects of policy uncertainty and risk aversion may be more pronounced. It could also be valuable to apply our models to different case studies beyond the Texas-Louisiana Gulf Coast. This would help confirm whether our findings hold more generally or include some elements that are specifically linked to the unique features of this case study. Lastly, we could extend the models to be able to

consider alternate policy designs for promoting CCUS infrastructure development. For example, we could study combinations of upfront incentives for CCUS infrastructure investments and ongoing incentives for CO<sub>2</sub> capture.

## Acknowledgments

The work described in this paper was supported by a grant from the Alfred P. Sloan Foundation to The University of Texas at Austin, titled “The Economics of Scaling Carbon Capture, Utilization, and Storage.”

## References

- Carneiro, J., Martinez, R., Suárez, I., Zarhloule, Y., Rimi, A., 2015. Injection rates and cost estimates for CO<sub>2</sub> storage in the west Mediterranean region. *Environmental Earth Sciences* 73, 2951–2962.
- Electric Power Research Institute, 2022. LCRI Net-Zero 2050: U.S. Economy-Wide Deep Decarbonization Scenario Analysis. Technical Report.
- EPA, 2022. EPA Facility Level GHG Emissions Data. URL: <https://ghgdata.epa.gov/ghgp/main.do>.
- Fuss, S., Szolgayova, J., Obersteiner, M., Gusti, M., 2008. Investment under market and climate policy uncertainty. *Applied Energy* 85, 708–721.
- Global CCS Institute, 2022. Global Status of CCUS 2022. Technical Report.
- International Energy Agency, 2011. The Costs of CO<sub>2</sub> Storage: Post-demonstration CCS in the EU. Technical Report.
- International Energy Agency, 2019. World Energy Outlook. Technical Report.
- International Energy Agency, 2020. The role of CCUS in low-carbon power systems. Technical Report.
- IPCC, 2022. Summary for policymakers, in: Pörtner, H.O., Roberts, D.C., Tignor, M.M.B., Poloczanska, E.S., Mintenbeck, K., Alegría, A., Craig, M., Langsdorf, S., Löschke, S., Möller, V., Okem, A., Rama, B. (Eds.), *Climate Change 2022: Impacts, Adaptation and Vulnerability. Contribution of Working Group II to the Sixth Assessment Report of the Intergovernmental Panel on Climate Change*. Cambridge University Press.
- Jones, E.C., Yaw, S., Bennett, J.A., Ogland-Hand, J.D., Strahan, C., Middleton, R.S., 2022. Designing multi-phased CO<sub>2</sub> capture and storage infrastructure deployments. *Renewable and Sustainable Energy Transition* 2, 100023.
- Kriegler, E., Weyant, J.P., Blanford, G.J., Krey, V., Clarke, L., Edmonds, J., Fawcett, A., Luderer, G., Riahi, K., Richels, R., Rose, S.K., Tavoni, M., Van Vuuren, D.P., 2014. The role of technology for achieving climate policy

- objectives: overview of the EMF 27 study on global technology and climate policy strategies. *Climatic Change* 123, 353–367.
- Kuby, M.J., Bielicki, J.M., Middleton, R.S., 2011. Optimal Spatial Deployment of CO<sub>2</sub> Capture and Storage Given a Price on Carbon. *International Regional Science Review* 34, 285–305.
- Lee, S.Y., Lee, J.U., Lee, I.B., Han, J., 2017. Design under uncertainty of carbon capture and storage infrastructure considering cost, environmental impact, and preference on risk. *Applied Energy* 189, 725–738.
- Luh, S., Budinis, S., Giarola, S., Schmidt, T.J., Hawkes, A., 2020. Long-term development of the industrial sector – Case study about electrification, fuel switching, and CCS in the USA. *Computers & Chemical Engineering* 133, 106602.
- Mendelevitch, R., Herold, J., Oei, P.y., Tissen, A. (Eds.), 2010. CO<sub>2</sub> highways for Europe: modelling a carbon capture, transport and storage infrastructure for Europe. Number 340 in CEPS working document, CEPS, Brussels.
- Middleton, R.S., 2013. A new optimization approach to energy network modeling: anthropogenic CO<sub>2</sub> capture coupled with enhanced oil recovery: A new optimization approach to energy network modeling. *International Journal of Energy Research* 37, 1794–1810.
- Middleton, R.S., Bielicki, J.M., 2009. A scalable infrastructure model for carbon capture and storage: SimCCS. *Energy Policy* 37, 1052–1060.
- Middleton, R.S., Kuby, M.J., Wei, R., Keating, G.N., Pawar, R.J., 2012. A dynamic model for optimally phasing in CO<sub>2</sub> capture and storage infrastructure. *Environmental Modelling & Software* 37, 193–205.
- Middleton, R.S., Yaw, S., 2018. The cost of getting CCS wrong: Uncertainty, infrastructure design, and stranded CO<sub>2</sub>. *International Journal of Greenhouse Gas Control* 70, 1–11.
- Morbee, J., Serpa, J., Tzimas, E., 2011. Optimal planning of CO<sub>2</sub> transmission infrastructure: The JRC InfraCCS tool. *Energy Procedia* 4, 2772–2777.
- National Energy Technology Laboratory, 2015. National Carbon Sequestration Database and Interactive Viewer (NATCARB). URL: <https://www.netl.doe.gov/coal/carbon-storage/strategic-program-support/natcarb-atlas>.
- National Petroleum Council, 2019. Meeting The Dual Challenge: A Roadmap to At-Scale Deployment of Carbon Capture, Use, And Storage. Technical Report 1.
- Rogelj, J., Luderer, G., Pietzcker, R.C., Kriegler, E., Schaeffer, M., Krey, V., Riahi, K., 2015. Energy system transformations for limiting end-of-century warming to below 1.5 °C. *Nature Climate Change* 5, 519–527.

- Smith, E.E., 2021. The Cost of CO<sub>2</sub> Transport and Storage in Global Integrated Assessment Modeling. Ph.D. thesis. Massachusetts Institute of Technology.
- Tutton, P., 2018. Carbon Capture and Storage Network Optimization Under Uncertainty. Thesis. University of Texas at Austin. Austin, Tx, USA.
- Wang, H., Chen, W., Zhang, H., Li, N., 2020. Modeling of power sector decarbonization in China: comparisons of early and delayed mitigation towards 2-degree target. *Climatic Change* 162, 1843–1856.
- Waxman, A.R., Corcoran, S., Robison, A., Leibowicz, B.D., Olmstead, S., 2021. Leveraging scale economies and policy incentives: Carbon capture, utilization & storage in Gulf clusters. *Energy Policy* 156, 112452.
- White House, 2016. United States Mid-Century Strategy for Deep Decarbonization. Technical Report.
- White House, 2021. Council on Environmental Quality Delivers Report to Congress on Steps to Advance Responsible, Orderly, and Efficient Development of Carbon Capture, Utilization, and Sequestration | CEQ.